Proteomics Characterization of Mouse Kidney Peroxisomes by Tandem Mass Spectrometry and Protein Correlation Profiling*[S]

Sebastian Wiese‡§, Thomas Gronemeyer‡§, Rob Ofman¶, Markus Kunze‖, Cláudia P. Grou**, José A. Almeida**, Martin Eisenacher‡, Christian Stephan‡, Heiko Hayen‡‡, Lukas Schollenberger§§, Thomas Korosec‖, Hans R. Waterham¶, Wolfgang Schliebs¶¶, Ralf Erdmann¶¶, Johannes Berger‖, Helmut E. Meyer‡, Wilhelm Just§§, Jorge E. Azevedo**, Ronald J. A. Wanders¶, and Bettina Warscheid‡‖‖

The peroxisome represents a ubiquitous single membrane-bound key organelle that executes various metabolic pathways such as fatty acid degradation by α- and β-oxidation, ether-phospholipid biosynthesis, metabolism of reactive oxygen species, and detoxification of glyoxylate in mammals. To fulfil this vast array of metabolic functions, peroxisomes accommodate ~50 different enzymes at least as identified until now. Interest in peroxisomes has been fueled by the discovery of a group of genetic diseases in humans, which are caused by either a defect in peroxisome biogenesis or the deficient activity of a distinct peroxisomal enzyme or transporter. Although this research has greatly improved our understanding of peroxisomes and their role in mammalian metabolism, deeper insight into biochemistry and functions of peroxisomes is required to expand our knowledge of this low abundance but vital organelle. In this work, we used classical subcellular fractionation in combination with MS-based proteomics methodologies to characterize the proteome of mouse kidney peroxisomes. We could identify virtually all known components involved in peroxisomal metabolism and biogenesis. Moreover through protein localization studies by using a quantitative MS screen combined with statistical analyses, we identified 15 new peroxisomal candidates. Of these, we further investigated five candidates by immunocytochemistry, which confirmed their localization in peroxisomes. As a result of this joint effort, we believe to have compiled the so far most comprehensive protein catalogue of mammalian peroxisomes. ***Molecular & Cellular Proteomics 6:2045–2057, 2007.***

From the ‡Medizinisches Proteom-Center, Ruhr-Universitaet Bochum, Universitaetsstrasse 150, 44780 Bochum, Germany, ¶Department of Clinical Chemistry, Academic Medical Center, University of Amsterdam, P. O. Box 22700, 1100 DE Amsterdam, The Netherlands, ‖Center for Brain Research, Medical University of Vienna, A-1090 Vienna, Austria, **Instituto de Biologia Molecular e Celular (IBMC), Rua do Campo Alegre, 823, 4150-180 Porto, Portugal and Instituto de Ciências Biomédicas de Abel Salazar (ICBAS), Universidade do Porto, Largo do Prof. Abel Salazar, 2, 4099-003 Porto, Portugal, ‡‡Institute for Analytical Sciences (ISAS), Bunsen-Kirchhoff-Str. 11, 44139 Dortmund, Germany, §§Biochemie-Zentrum der Universitaet Heidelberg (BZH), Im Neuenheimer Feld 328, 69120 Heidelberg, Germany, and ¶¶Abteilung fuer Systembiochemie, Medizinische Fakultaet der Ruhr-Universitaet Bochum, 44780 Bochum, Germany

Received, April 13, 2007, and in revised form, July 20, 2007
Published, MCP Papers in Press, September 2, 2007, DOI 10.1074/mcp.M700169-MCP200

Peroxisomes are small organelles present in virtually all eukaryotic cells. They are surrounded by a single membrane and harbor a large set of enzymes that enables them to execute an array of metabolic functions, such as α- and β-oxidation of fatty acids, ether-phospholipid biosynthesis, metabolism of reactive oxygen species, and detoxification of glyoxylate in mammals (1). The biogenesis of peroxisomes includes complex processes such as membrane assembly, import of matrix proteins, and division of mature peroxisomes. These processes require the concerted action of a subcellular machinery composed of more than 20 different proteins, the so-called peroxins (2, 3). Failure in the biogenesis of peroxisomes or deficiencies in the function of single peroxisomal proteins leads to serious diseases in humans, such as Zellweger syndrome and X-linked adrenoleukodystrophy (1). Although much has been learned about peroxisomes in recent years, crucial aspects of their functional activities and biogenesis still remain a conundrum.

The combination of subcellular fractionation and mass spectrometric analysis, referred to as organellar proteomics (for reviews, see Refs. 4–6), is a powerful method that facilitates the comprehensive characterization of subcellular structures, such as peroxisomes. However, the low abundance of peroxisomes combined with the limited ability to purify this organelle has complicated the proteomics analysis of peroxisomes until now (7). Several proteomics studies have been performed on peroxisomes from *Saccharomyces cerevisiae* cultured in oleate-containing medium which induces the formation of peroxisomes (8–10). To isolate peroxisomes with high purity and in adequate yields from mammalian cells, Kikuchi *et al.* (11) performed density gradient centrifugation of rat liver preparations using Nycodenz followed by immunoaffinity purification using an antibody against the abundant per-

oxisomal membrane protein (PMP)[1] 70. Proteomics analysis of these peroxisomal preparations by SDS-PAGE followed by LC/tandem MS resulted in the identification of more than 50 *bona fide* constituents as well as a new isoform of Lon protease. Further studies of rat liver peroxisomes using two-dimensional gel electrophoretic techniques and MS led to the identification of microsomal glutathione *S*-transferase (12) as well as nudix hydrolase 19, referred to as RP2 (13). In addition, the known microsomal proteins aldehyde dehydrogenase, cytochrome b_5, and its corresponding reductase were detected in peroxisomal preparations from rat liver (11, 12). However, no information on the origin of these proteins (*i.e.* whether they are derived from peroxisomes or potentially co-purified microsomes) was provided by the descriptive proteomics strategies applied in these studies. To address this important issue, Aitchison and co-workers (10) introduced a relative quantitative MS-based proteomics approach to determine the enrichment or depletion of proteins detected in two peroxisomal membrane preparations from yeast that differed in their degree of purity. By determining the abundance ratios of the proteins identified in these two fractions, they were able to identify new peroxisome-associated proteins. At about the same time, strategies were developed to enable the profiling of hundreds of proteins through various fractions of a density gradient using quantitative MS in combination with (14) or without (15) stable isotope labels. These quantitative profiling approaches combined with statistical analyses were shown to allow for the reliable cellular location of proteins in a global manner, thereby providing an excellent means by which new insights into the proteomes and functions of subcellular structures can be obtained (15–19).

In the present work, we report the proteomics characterization of mammalian peroxisomes. We used differential and Nycodenz density gradient centrifugation to isolate peroxisomes from mouse kidney with high purity. Application of MS-based proteomics methodologies enabled the identification of virtually all known resident proteins of the matrix as well as the membrane compartment of mammalian peroxisomes. Moreover through localization studies by protein correlation profiling combined with statistical analyses, we identified 15 new candidate peroxisomal proteins in mouse kidney. The presence of five of these candidate proteins (zinc-binding alcohol dehydrogenase domain-containing protein 2, acyl-coenzyme A dehydrogenase family member 11, acyl-CoA-binding protein 5, the RIKEN cDNA clone 2810439K08 designated here as PMP52, and MOCO sulfurase C-terminal domain-containing 2 protein) in peroxisomes was confirmed by *in vivo* studies. Although the first three proteins appear to reside in the matrix and PMP52 is in all likelihood a new integral membrane component of mammalian peroxisomes of unknown function, the latter protein was shown to be localized in both peroxisomes and mitochondria. As a result, we believe to have compiled the so far most comprehensive catalogue of mammalian peroxisomes.

EXPERIMENTAL PROCEDURES

Purification of Peroxisomes from Mouse Kidney—Peroxisomes were purified from kidneys of male Swiss mice, 4–6 months of age, as described previously (13). In brief, this method involves homogenization of kidneys in a buffer containing 10 mM MOPS-NaOH, 250 mM sucrose, 2 mM EDTA, and 0.1% ethanol (final pH = 7.4) followed by centrifugation of the homogenate at 600 × *g* for 10 min at 4 °C to produce a postnuclear supernatant. Peroxisomes were isolated by Nycodenz equilibrium gradient centrifugation as described previously (20). Fractions of 2 ml were taken from the bottom of the gradient and assayed for the marker enzymes catalase (peroxisomes), glutamate dehydrogenase (mitochondria), β-hexosaminidase (lysosomes), and esterase (microsomes) as described previously (Ref. 13 and references therein). Highest activities for catalase and glutamate dehydrogenase were measured in gradient fractions 3 and 12, respectively. The remaining two enzymes showed highest activities in fractions 15–17 (Supplemental Fig. 2A). The protein concentrations were measured according to Bradford (21) using BSA as standard. Peroxisome pellets were prepared from the peroxisomal peak fraction (fraction 3) by centrifugation at 16,000 × *g* for 10 min and stored at −80 °C. For protein correlation profiling, 1-ml aliquots of gradient fractions 2, 3, 4, 6, 8, and 10 were taken to prepare peroxisome pellets. Prior to proteomics analysis, pellets were resuspended in sample buffer containing 30 mM Tris-HCl, 2 M thiourea, and 7 M urea (pH 8.5) to a final protein concentration of about 1 μg/μl.

Purification of Peroxisomal Membranes from Mouse Kidney—Peroxisomal membranes were prepared by alkaline extraction as described previously (22). Briefly purified peroxisomes were resuspended in 0.12 M Na_2CO_3, pH 11.5, placed on ice for 30 min, and centrifuged at 100,000 × *g* (T1270, Sorvall®) for 1 h at 4 °C. Membrane pellets were then subjected to SDS-PAGE or in-solution tryptic digestion.

Western Blotting—Immunoblot analyses were performed as described elsewhere (23). Briefly sample aliquots of gradient fractions from mouse kidney were mixed with an equal volume of Laemmli buffer, resolved by 10% SDS-PAGE, and blotted onto a nitrocellulose membrane. Nonspecific binding sites were blocked for 1 h using a PBS solution containing 1 g/liter Tween 20 (PBST) supplemented with 3% BSA (w/v). Incubations of primary antibodies and secondary antibody (goat anti-rabbit IgG coupled to alkaline phosphatase) were performed in PBST with 3% BSA (w/v). After each incubation step, the blots were washed extensively in PBST. Antigen-antibody complexes were visualized using alkaline phosphatase staining in a buffer containing 0.1 M Tris-HCl (pH 9.5), 0.1 M NaCl, 5 mM $MgCl_2$, 0.33 g/liter 4-nitroblue tetrazolium chloride, and 0.17 g/liter 5-bromo-4-chloro-3-indolyl phosphate (disodium salt). The primary antibody for acyl-CoA dehydrogenase family member 11 was raised in rabbits against recombinant human protein as described previously (24). The primary antibodies against catalase, voltage-dependent anion-selective channel protein 1, and per-

[1] The abbreviations used are: PMP, peroxisomal membrane protein; GPF, gas-phase fractionation; IPI, International Protein Index; PCP, protein correlation profiling; SIM, selected ion monitoring; FA, formic acid; 3D, three-dimensional; PBE, peroxisomal bifunctional enzyme; EGFP, enhanced green fluorescent protein; ALDP, adrenoleukodystrophy protein; PEX, peroxin; ER, endoplasmic reticulum; ABC, ATP-binding cassette; ALDR, adrenoleukodystrophy-related; BACAT, bile acid-CoA:amino acid *N*-acyltransferase; PTS1, peroxisomal targeting signal type 1; FALDH, fatty aldehyde dehydrogenase; HCT, high capacity trap; LTQ, linear trap quadrupole; MOCO, molybdenium cofactor; MOSC, molybdenium cofactor sulfurase; AAA, ATPases associated with various cellular activities.

oxisomal membrane protein 70 were purchased from Biodesign International (Kennebunkport, ME), Santa Cruz Biotechnology (Santa Cruz, CA), and Sanbio (Beutelsbach, Germany), respectively.

Gel Electrophoresis and In-gel Digestion—For SDS-PAGE, 25 μl of 4× SDS sample buffer were added to 75 μl of protein sample. Proteins were separated on a polyacrylamide gel (15.2% total acrylamide, 1.3% bisacrylamide) with a 4% stacking gel using a Desaphor VA 300 system (Invitrogen) according to the manufacturer's instructions and subsequently stained by colloidal Coomassie Brilliant Blue G-250. The gel was equally cut in 2-mm slices. Gel bands were destained by alternately incubating them with 20 μl of 10 mM ammonium hydrogen carbonate (NH_4HCO_3) and 20 μl of 5 mM NH_4HCO_3, 50% ACN (v/v) for 10 min each. In-gel digestion was performed overnight at 37 °C using trypsin dissolved in 10 mM NH_4HCO_3 buffer (pH 7.8). The resulting peptides were extracted twice with 10 μl of ACN, 5% FA (50:50, v/v), and the resulting extracts were combined before ACN was removed *in vacuo*. For LC/MS analysis, samples were acidified by addition of 5% FA to a final volume of 20 μl.

In-solution Digestion—Protein samples were dissolved in 50 mM NH_4HCO_3 to a final concentration of 0.1 μg/μl. Then trypsin was added to result in a protein-to-trypsin ratio of 1:30, and enzymatic digestion was carried out for 6 h at 37 °C. For LC/MS analysis, the resulting peptide mixtures were diluted in 5% FA to 0.067 μg/μl.

Nano-HPLC/ESI-MS²—On-line reversed-phase capillary HPLC separations were performed using the Dionex LC Packings HPLC systems (Dionex LC Packings, Idstein, Germany) as described previously (25). ESI-MS² was performed on a Bruker Daltonics HCT plus ion trap instrument (Bremen, Germany) equipped with a nanoelectrospray ion source (Bruker Daltonics) and distal coated SilicaTips (FS360-20-10-D; New Objective, Woburn, MA). The instrument was externally calibrated with standard compounds. The general mass spectrometric parameters were as follows: capillary voltage, 1400 V; plate offset, 500 V; dry gas, 10.0 liters/min; dry temperature, 160 °C; aimed iou charge control, 150,000; maximal fill time, 500 ms. For MS² peptide analyses, data-dependent software (HCT plus, Esquire Control, Bruker Daltonics) was used. To generate fragment ions, low energy CID was performed on isolated multiply charged peptide ions with a fragmentation amplitude of 0.6 V. Exclusion limits were automatically placed on previously selected mass-to-charge ratios for 1.2 min. For tryptic peptide mixtures of comparably low complexity, (i) MS spectra were a sum of seven individual scans ranging from *m/z* 300 to 1500 with a scanning speed of 8100 (*m/z*)/s and (ii) MS² spectra were a sum of four scans ranging from *m/z* 100 to 2200 at a scan rate of 26,000 (*m/z*)/s. For complex peptide mixtures, both MS and MS² spectra were a sum of two individual scans. A second series of MS² experiments was performed on a 7-tesla Finnigan LTQ-FT (Thermo Electron, Bremen, Germany) instrument equipped with a nanoelectrospray ion source. The instrument was operated in the data-dependent mode for MS and MS² analyses similar to the method described by Olsen *et al.* (26). Briefly survey MS spectra from *m/z* 300 to 1500 were acquired in the FTICR cell with $r = 25{,}000$ at *m/z* 400 with a target accumulation value of 50,000,000. The three most intense ions were sequentially isolated for accurate mass measurements by an FTICR "selected ion monitoring (SIM) scan" (mass window, ±5 Da; resolution of 50,000; and target accumulation value of 100,000). Subsequent fragmentation was carried out in the linear ion trap by low energy CID (target accumulation value of 10,000). Former target ions selected for MS/MS were dynamically excluded for 45 s. The total cycle time was ~3 s. The general mass spectrometric parameters were as follows: spray voltage, 1.8 kV; no sheath and auxiliary gas flow; ion transfer tube temperature, 200 °C; and normalized collision energy of 35% for MS² with activation $q = 0.25$ and activation time of 30 ms. Ion selection thresholds were 1000 counts for MS and 500 counts for MS². In general, we performed gas-phase fractionation in the *m/z* dimension for precursor ion selection (GPF($P^+_{m/z}$)) in MS/MS scans. To this end, each sample was analyzed thrice with a *m/z* range of 300–1500 in the MS scan but each time with different overlapping narrow *m/z* ranges covering 400–650, 600–850, and 800–1200 for the selection of precursor ions in MS² scans.

Mass Spectrometric Data Analysis—Peak lists of MS² spectra acquired on the HCT ion trap (Bruker Daltonics) and LTQ-FT (Thermo Electron) instrument were generated using the software tools DataAnalysis 3.3 and Bioworks 3.1 SR 1, respectively. In either case, default parameters were used for the generation of peak lists. For peptide and protein identification, peak lists were correlated with the mouse International Protein Index (mouse IPI version 3.15.1) (www.ebi.ac.uk) database containing 68,222 protein entries using MASCOT (release version 2.0.04) (27). Species restriction in database searches to mouse was justified by the fact that peroxisomal preparations from mouse kidney were analyzed. All searches were performed with tryptic specificity allowing two missed cleavages. Oxidation of methionine was considered as variable modification. MS² spectra acquired on the HCT ion trap instrument (Bruker Daltonics) were generally accepted with a MASCOT cutoff score of 22.5 as well as mass tolerances of 1.2 and 0.4 Da for MS and MS² experiments, respectively. LTQ-FT mass spectra were searched with a mass tolerance of 2 ppm for precursor ions and 0.4 Da for fragment ions, and MS² spectra were accepted with a minimum MASCOT score of 15. Cutoff scores applied in this work provided the highest number of protein identifications on the basis of two peptides and a false positive rate below 5%. False positive rates were calculated as described previously (28). In brief, the exported mass spectra were searched using MASCOT (release version 2.0.04) against a composite database consisting of the mouse IPI and a duplicate of the same database in which the amino acid sequence of each protein entry was randomly shuffled. Proteins were assembled on the basis of peptide identifications using the ProteinExtractor Tool (version 1.0) in ProteinScape (version 1.3, Bruker Daltonics) and sorted according to their identification scores. This software automatically removes redundancies in protein entries, *i.e.* only the protein of lowest molecular weight is reported. In the case that different isoforms of a protein were reported by ProteinExtractor, these protein entries were inspected manually, *i.e.* the presence of each protein isoform was confirmed by the identification of at least one unique peptide. In the case that no unique peptide could be reliably identified, the respective isoform of the protein was not reported. Subsequent to the assembly of proteins, the false positive rate was calculated as the quotient of the number of all proteins identified in the shuffled database and the sum of all protein identifications in both the mouse IPI database and its shuffled version. Protein hits up to an accumulated false positive rate of 5% were considered as true positive protein identifications. In the case of database searches using LTQ-FT-MS² datasets, no false positive hits were detected when proteins were identified on the basis of at least two peptides with a minimum MASCOT score of 15. UniProt (www.pir.uniprot.org) and Harvester (harvester.embl.de) search engines were then used to annotate proteins identified by MS.

For protein correlation profiling, the acquired nano-HPLC/LTQ-FT-MS² runs were correlated using the software package DeCyder MS (version 1.0; GE Healthcare). Peptide peaks were detected with an average peak width of 0.5 min using the Pepdetect Module. Subsequently peak matching was performed with a mass accuracy of at least 0.01 Da and a maximum time window of 4 min using the PepMatch software module. Following the matching of peptide peaks, peptide abundances in each of the analyzed gradient fractions were calculated from the area under the peak. All data processing steps were manually inspected to ensure correct peak detection and matching; overlapping peaks were discarded. MS² spectra within a range of 20% to the peak area were linked to those peaks and

exported for a secondary search using the SEQUEST™ algorithm (SEQUEST version 3.0) (29) with the same parameters as stated above, although a cutoff Metascore of 3.0 was applied as calculated by ProteinScape (version 1.3, Bruker Daltonics) as described previously (28). To generate protein correlation profiles, normalized abundance profiles of all peptides assigned to a given protein in the different gradient fractions analyzed were averaged. Abundance profiles were normalized by setting the highest intensity measured for a given peptide in the selected gradient fractions to one. "χ^2 values" were calculated with the formula $\chi^2 = \sum_i (x_i - x_p)^2/x_p$ in which i is the fraction number, x_i is the normalized value in fraction i, and x_p is the value of the reference protein in fraction i. The peroxisomal bifunctional enzyme (PBE), the mitochondrial ATP translocase, and peroxiredoxin-5 as bilocalized protein were used as reference proteins. In a second approach, all protein profiles obtained were partitioned into k clusters of similar shape (30). This was done in an iterative procedure in which cluster centers and cluster memberships were changed until convergence was reached or a maximum number of iterations were performed. Initially cluster centers were randomly distributed, and each protein was assigned to the cluster with the smallest distance to the cluster center. However, cluster centers were moved dependent on the current cluster members (using one of several possible centroid calculation methods) in each iteration step. This led to a new assignment of cluster memberships. In general, the process has converged if both cluster centers and cluster membership do not change anymore. Depending on the start conditions, convergence may not be reached. Genedata Expressionist (Genedata AG, Basel, Switzerland) was used on all protein profiles with "Euclidean" distance function and with "mean" as the centroid calculation method. The input parameter k determines the number of clusters created. In this work, "maximal iterations" was set to 50. Because all measurements were given, no "missing values" had to be considered.

Cell Culture and Immunofluorescence Microscopy—COS7 cells (ATCC CRL-1651) were cultivated in Dulbecco's modified Eagle's medium with 10% fetal calf serum, 2 mM L-glutamine, 50 units/ml penicillin, and 100 μg/ml streptomycin (BioWhittaker, Walkersville, MD). COS7 cells were transfected with plasmids by electroporation using Gene Pulser II (Bio-Rad) with the settings 200 mV and 950 microfarads. Cells were grown on glass coverslips for 48 h and then fixed for 20 min with 4% paraformaldehyde in PBS (137 mM NaCl, 2.7 mM KCl, 8.1 mM $Na_2HPO_4 \times 2H_2O$, and 1.46 mM KH_2PO_4). Afterward cells were washed with PBS, permeabilized with 0.1% Triton X-100 in PBS, and blocked with blocking solution (PBS containing 10% FCS and 5 μg/ml BSA). Rabbit antibodies against EGFP (1:800) and PMP70 (1:2000; Affinity BioReagents, Golden, CO) as well as mouse antibodies against EGFP (1:800; Chemicon, Temecula, CA), FLAG (1:800, M2, Sigma), and MYC (1:200, 9E10; ATCC CRL-1729) were diluted in blocking solution. Cells were incubated with primary antibodies for 2.5 h. Cy2- or Cy3-coupled secondary antibodies against mouse or rabbit immunoglobulins (1:150; Jackson ImmunoResearch Laboratories, Suffolk, UK) were also diluted in blocking solution and added for 1 h. For MitoTracker staining, cells were kept in Dulbecco's modified Eagle's medium containing all components and MitoTracker (1:10,000; Invitrogen) for 1 h prior to fixation with paraformaldehyde and were then processed as described above. Cells were analyzed using an Olympus BX51 fluorescence microscope.

RESULTS

Proteomics Investigation of Mouse Kidney Peroxisomes—Peroxisomes from mouse kidney were isolated by density and gradient centrifugation of a light mitochondrial fraction prepared by differential centrifugation using established protocols (13). The protein composition of the peroxisomal peak fraction (fraction 3) as determined by both enzyme activity and Western blot analyses against organelle marker proteins (Supplemental Fig. 2) was analyzed by MS-based proteomics methodologies. To increase the effective dynamic range of MS analyses, both SDS-PAGE separation and gas-phase fractionation in the m/z dimension for precursor ion selection (GPF($P^+_{m/z}$)) were used as described under "Experimental Procedures." In addition, we prepared an enriched membrane fraction of purified peroxisomes by alkaline treatment (Na_2CO_3, pH 11.5) to facilitate the identification of peroxisomal membrane proteins of low abundance by proteomics means. After SDS-PAGE separation of peroxisomal samples and in-gel tryptic digestion of proteins, nano-HPLC/ESI-MS^2 analyses were performed on a 3D ion trap instrument. For GPF($P^+_{m/z}$) enhanced nano-HPLC/ESI-MS^2 analyses of tryptic digests of mouse kidney peroxisomes we used both a 3D ion trap and a hybrid LTQ-FTMS system. On the latter instrument, we performed SIM as described previously (26). GPF in the m/z dimension ($GPF_{m/z}$) in MS scans was used previously to characterize the proteome of yeast peroxisomes by tandem MS (9). To effectively increase the rate of peptide sampling, we tested different conditions for GPF($P^+_{m/z}$) (data not shown), which resulted in the design of three slightly overlapping m/z windows of 400–650, 600–850, and 800–1200. For protein assembly, uniform MS^2 datasets from both gel-enhanced and GPF($P^+_{m/z}$) analyses were generated and then correlated with a composite version of the IPI database using MASCOT (28). Proteins were identified on the basis of at least two peptides with a false positive rate below 5%. No false positive hits occurred when LTQ-FT-MS^2 datasets were analyzed under the conditions described here. Table I provides a compiled overview of all MS-based proteomics investigations conducted in this work to establish a comprehensive catalogue of proteins of mouse kidney peroxisomes (for detailed information on protein identification results and intracellular localization refer to Supplemental Table 1). Taken together, proteomics analyses resulted in the identification of 252 nonredundant proteins, 64 proteins (25%) of which were reported in the literature to be localized in kidney peroxisomes. The percentage of peroxisomal proteins in each analysis was in the range of 35–48. Of the 64 peroxisomal proteins identified, 42 are known peroxisomal matrix proteins, whereas 22 were PMPs (Table I). Although most PMPs could already be identified through proteomics analysis of peroxisome preparations without further enrichment of membranes using SDS-PAGE followed by tandem MS analysis, four integral components of the peroxisomal membrane of very low abundance could only be detected in the respective membrane preparations. These membrane proteins were the murine adrenoleukodystrophy protein (ALDP) (31), Mpv17-like protein (32), and the two peroxins PEX13 (33) and PEX2 (34) (Supplemental Table 1). PEX13 was reported previously to represent not more than 0.1% of total protein of mammalian peroxisomes (35, 36), and the amount of ALDP was estimated to be less than 1/70 of the

TABLE I

Proteins and their subcellular localization identified in peroxisomes and enriched peroxisomal membrane samples from mouse kidney by mass spectrometry-based proteomics methodologies

Numbers in parentheses represent total spectral counts of each group of proteins.

	Intact peroxisomes				Peroxisomal membranes		Total
	SDS-PAGE/3D ion trap	GPF($P^+_{m/z}$)[a] 3D ion trap	GPF($P^+_{m/z}$)[a] LTQ-FTMS	GPF($P^+_{m/z}$)[a] LTQ-FTMS[b]	SDS-PAGE 3D ion trap	GPF($P^+_{m/z}$)[a] LTQ-FTMS	
Total number of MS/MS spectra searched	42,328	12,106	8,802	6,520	28,255	2,437	100,448
Number of identified proteins	135	91	102	114	136	80	252
Swiss-Prot annotation							
Number of proteins with known cellular localization	110	77	84	94	106	64	187
Number of proteins with unknown localization	25 (867)	14 (73)	21 (145)	24 (176)	32 (629)	17 (93)	65
Number of known peroxisomal proteins	47 (4,455)	39 (832)	49 (1,196)	53 (1,759)	47 (2,018)	33 (328)	64
Peroxisomal matrix proteins	34 (4,157)	31 (736)	39 (1,140)	39 (1,703	29 (1,529)	24 (252)	42
Peroxisomal membrane proteins	13 (155)	8 (96)	10 (56)	14 (56)	18 (489)	10 (76)	22
Of these colocalized with other organelle	8	7	3	5	8	1	8
Number of mitochondrial proteins	16 (198)	10 (113)	6 (59)	7 (65)	15 (118)	9 (38)	31
Number of cytoplasmic proteins	22 (444)	10 (92)	10 (85)	10 (96)	8 (61)	5 (16)	30
Number of ER proteins	4 (78)	4 (38)	4 (31)	7 (45)	14 (261)	7 (35)	27
Number of proteins from other organelles	13 (268)	7 (24)	8 (47)	10 (18)	11 (65)	7 (36)	35
Percentage of peroxisomal proteins (%)	35	43	48	46	35	41	25

[a] Gas-phase fractionation in the *m/z* dimension for selection of precursor ions.

[b] Peroxisomal peak fraction analyzed in protein correlation profiling experiments.

amount of PMP70 in rat liver (37).

Due to the fact that peroxisomes cannot be purified to homogeneity, we also identified a total of 123 proteins (49%) that localize to subcellular structures other than peroxisomes. However, the percentage of these most likely contaminating proteins in each analysis was only 34 on average, indicating that these proteins were of rather low abundance in the peroxisomal samples analyzed here. To substantiate this observation, we obtained information on the abundance of individual proteins identified in the peroxisome preparations by peptide counting (38) (Table I and Supplemental Table 1). On average, 75% of all spectral counts were assigned to the 64 peroxisomal proteins identified in mouse kidney peroxisomes in this work, whereas only 16% were assigned to the 123 proteins known to localize to other subcellular structures. Accordingly the 65 proteins of unknown localization (26% of all identified proteins) contributed to 9% of total spectral counts on average. On the basis of spectral counts we can further report that alkaline treatment of peroxisome preparations increased the abundance of peroxisomal membrane proteins ~3-fold accompanied by a decrease of about 50% in both abundance and number of cytoplasmic proteins. Abundances of ER proteins and mitochondrial proteins were lower than 10% each.

For a current, most comprehensive proteome catalogue of mouse kidney peroxisomes including all 64 peroxisomal proteins identified in this work plus information on gene name, accession numbers, and general function please see Supplemental Table 2. In addition, we identified 65 proteins of so far unknown localization in preparations of mouse kidney peroxisomes. We assume that the latter set may contain new potential candidates of mammalian peroxisomes.

Localization by Protein Correlation Profiling—To reliably identify genuine proteins of peroxisomes, we performed protein correlation profiling (PCP) (15). In this semiquantitative MS approach, the distribution of proteins across a gradient are compared by plotting the normalized peptide abundances against the respective gradient fractions. Proteins belonging to the same organelle feature similar profiles that show highest abundances in the corresponding organelle peak fraction. Consequently candidates with profiles that either follow or deviate from the profiles of true resident proteins of that organelle can thus be classified unambiguously. Proteins may also feature characteristics of protein profiles of two or more distinct subcellular structures, indicating dual or even multiple localization sites (17).

In the experimental design, we focused on the ability to reliably discriminate between genuine components of peroxisomes and other subcellular structures, in particular mitochondria, which are generally known to represent a major contaminant of peroxisomes purified by density and gradient centrifugation. To this end, consecutive peptide MS^2 analyses of six gradient fractions were performed on a nano-HPLC/ESI-LTQ-FTICR system using GPF($P^+_{m/z}$) combined with SIM scans. We analyzed two technical replicates, referred to as Set 1 and Set 2. A total of 3999 peptides were followed across the six fractions, allowing for the calculation of profiles for 110 of 114 proteins identified in the peroxisomal peak fraction (Supplemental Table 3).

We applied two independent statistical approaches to evaluate the protein profiles established in Set 1 and Set 2 and to eventually determine new genuine components of mouse kidney peroxisomes. We first compared the correlation profiles of peroxisomal proteins and typical contaminants, *i.e.* mitochondrial proteins, using the χ^2 method. In this supervised

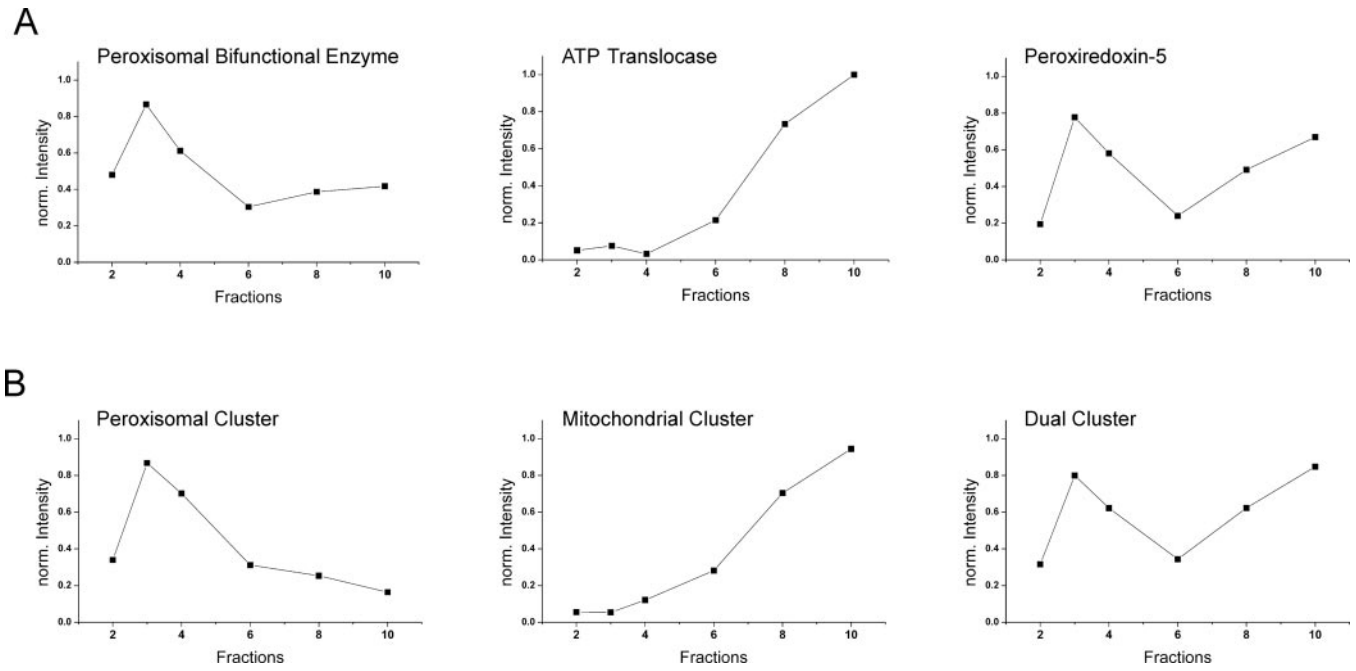

FIG. 1. **Protein correlation profiling to facilitate the identification of genuine components of mouse kidney peroxisomes against a background of contaminating proteins.** *A*, protein profiles established as an average of normalized (*norm.*) peptide abundances. Shown are the profiles of the marker proteins PBE, ATP translocase, and peroxiredoxin-5, which are known to localize to peroxisomes, mitochondria, and both organelles, respectively. The profile of the latter protein is representative for proteins that distribute between peroxisomes and another cellular compartment, such as mitochondria, referred to as dual localization in this work. *B*, average profiles of the peroxisomal, mitochondrial, and dual cluster obtained by hierarchical *k*-means clustering of protein profiles (Set 1) established in this work.

approach, the correlation values (χ^2 values) between the correlation profiles of marker proteins are calculated, and then a "goodness of fit" is defined for all other proteins. We chose the PBE, the mitochondrial ATP/ADP translocator, and the bilocalized protein peroxiredoxin-5 as marker proteins. The profiles established as an average of normalized peptide abundances of these marker proteins are shown in Fig. 1*A*. Correlation values were then calculated for all other proteins identified in the peroxisomal peak fraction for Set 1 and Set 2 (Supplemental Table 4). Peroxisomal and mitochondrial proteins clearly separated in their χ^2 values, indicating the ability to discriminate between these two groups of proteins. Generally proteins localized to peroxisomes exhibited great similarity to the profile of PBE (χ^2 values below 3) and greatly differed from the profile of ATP translocase (χ^2 values greater than 12). In contrast, mitochondrial proteins uniformly showed χ^2 values lower than 8 when compared with the profile of ATP translocase. Because the established profiles of PBE and peroxiredoxin-5 showed great similarity in the first three fractions (fractions 2, 3, and 4) whereas major differences only appeared in the gradient fractions of lower density (fractions 6, 8, and 10), their respective χ^2 values were rather similar (Fig. 1*A* and Supplemental Table 4). We therefore considered a protein as being localized exclusively in peroxisomes if the squared distance was smaller to PBE than to peroxiredoxin-5. In the opposite case, a dual localization was assigned to the respective protein.

To support the localization data obtained on the basis of normalized square deviations, we additionally used hierarchical *k*-means clustering as an unsupervised method (30). Briefly, the Euclidean distance between protein profiles was utilized to partition all profiles into *k* clusters of similar shape. This was done in an iterative procedure in which cluster centers and cluster memberships are updated until convergence or a maximum number of iterations is reached. In *k*-means clustering with $k = 1$ to $k = 6$, one large cluster is always found containing quite heterogeneous profiles, referred to as magnet cluster. Higher *k*-values do not partition the magnet cluster but partition the smaller clusters instead. We therefore used 2-means clustering and successively partitioned the larger or more heterogeneous cluster into two further subclusters, resulting in eight clusters with no further partitioning. The average profile shapes of these clusters were then classified into three groups (mitochondrial, peroxisomal, and dual location) based on our knowledge about profile shapes of organelle marker proteins. The average profile shapes of the three final clusters are shown in Fig. 1*B* (for information on cluster affiliations of individual proteins please refer to Supplemental Tables 3 and 4). Next we defined two additional criteria to clearly distinguish peroxisomal proteins from cytoplasmic and ER proteins in our datasets and hence to extract a most reliable list of genuine components of peroxisomes including new candidates. 1) The profile of a peroxisomal protein has to show a global maximum in the per-

oxisomal peak fraction 3 of the gradient, and 2) a protein considered as bilocalized has to show two local maxima in its respective profile with one maximum in fraction 3 and the other maximum in fraction 10. Proteins that did not meet all the criteria established here in Set 1 and/or Set 2 were designated as "false," and thus no localization was assigned (Supplemental Table 4). Only those proteins that were uniformly predicted to exhibit dual location in both datasets (Set 1 and Set 2) were reported as bilocalized proteins in this work.

Statistical analyses of Set 1 and Set 2 using two independent methods (*k*-means clustering and χ^2 method) in combination with the criteria established in this work resulted in the successful location of 87 proteins. Of these, 55 proteins were assigned to peroxisomes, 23 proteins were assigned to mitochondria, and nine proteins were assigned to a dual location (Supplemental Table 4). We note that protein location results obtained by *k*-means clustering and the χ^2 method were in very good agreement. For example, only seven proteins were predicted to localize to different subcellular structures using these two different statistical approaches in Set 1. In general, the difference in data was only between dual and peroxisomal or mitochondrial location because dual protein profiles display characteristics of both peroxisomal and mitochondrial profiles. Only three proteins (PEX11b, 2-hydroxyphytanoyl-CoA lyase, and tetratricopeptide repeat protein 11) known to localize to peroxisomes did not meet all the criteria in Set 1 and Set 2 and, thus, were finally designated as false. However, no known peroxisomal protein was assigned to mitochondrial location, indicating the high accuracy of this approach. As the final result of this effort, we could extract 11 new candidates most likely representing genuine components of mouse kidney peroxisomes as well as four proteins that appear to exhibit a dual location (Table II and Supplemental Table 4). Of the 15 candidates reported in this work, six were identified previously in rat liver peroxisomes by proteomics analysis (11, 12). With the exception of ACAD11, the RIKEN cDNA clone 1810022C23, and ACOT12, all reported candidates exhibited peptide counts below 10 (Table II), indicating that these proteins represent low abundance components of mouse kidney peroxisomes.

Validation by Fluorescence Microscopy—Proteomics investigations resulted in the identification of 15 candidates of mouse kidney peroxisomes (Table II). To corroborate MS-based results on protein localization studies, we analyzed the subcellular localization of selected proteins by immunofluorescence microscopy. Thus, fusion proteins of five candidates, namely the putative membrane proteins 2810439K08RIK (TMEM135 protein), referred to as PMP52 in this work, and MOCO sulfurase C-terminal domain-containing 2 protein (MOSC2) as well as the putative matrix proteins zinc-binding alcohol dehydrogenase domain-containing protein 2 (ZADH2), acyl-coenzyme A dehydrogenase family member 11 (ACAD11), and the acyl-CoA-binding protein 5 (ACBD5), were expressed in COS7 cells. Their subcellular localization was then investigated by co-localization with a peroxisomal (PMP70) and a mitochondrial (MitoTracker) marker. For PMP52 and the soluble proteins, a punctate pattern was observed that corresponds well to the pattern of the peroxisomal marker protein PMP70 (Fig. 2). As a control, mitochondria were detected with MitoTracker, but none of the proteins co-localized with mitochondria (Supplemental Fig. 1). MOSC2 could be shown to have a dual localization. Accordingly a MOSC2 variant carrying a C-terminal MYC tag was found in mitochondria but also in peroxisome (Fig. 2, *bottom*). However, when the MYC tag was fused to the N terminus and thus effectively blocked the predicted mitochondrial signal parts of the protein, MOSC2 was still found in peroxisomes, but no co-localization with mitochondria was observed (data not shown).

DISCUSSION

Subcellular fractionation combined with MS-based proteomics analysis provides a most powerful means to establish comprehensive protein catalogues of organelles. Because organelles are not static entities but rather dynamic cellular structures, the respective protein components can only be defined for a specific tissue, cell type, and/or metabolic state at a given time. A major benefit of organellar proteomics is that the complexity of an organelle-enriched sample is, in theory, compatible with the sensitivity and dynamic range of current MS-based methods, even allowing for the identification of proteins of low abundance. Yet thorough purification of subcellular structures remains a key factor in obtaining meaningful data in organellar proteomics. This is particularly true for mammalian peroxisomes, which contribute to only 1–5% of the cell volume depending on tissue type and metabolic state. Furthermore mitochondrial and ER membranes, which generally account for the largest fraction of total cellular membranes, may impede the detection of low abundance PMPs (36). This problem is further emphasized by the fact that PMPs only contribute to ~10% of the entire proteome of peroxisomes. Moreover although PMP70 and PMP22 are highly abundant in peroxisomal membranes (as a rough estimate 50% of total PMPs), peroxins such as PEX13 and PEX12 each account for less than 0.1% of total peroxisomal protein (35).

The current literature lists ~75 proteins as components of mouse kidney peroxisomes of which 48 reside in the matrix and 27 reside in the membrane. Of these, we identified 42 peroxisomal matrix and 22 peroxisomal membrane proteins (64 proteins in total, 85% coverage) by proteomics investigations of purified mouse kidney peroxisomes. We only failed to detect two ATP-binding cassette (ABC) transporters, two peroxins, and seven matrix proteins that were shown previously to localize to mammalian peroxisomes (Supplemental Tables 1 and 2).

Four ABC transporters, namely ALDP, adrenoleukodystrophy-related (ALDR) protein, PMP70, and PMP69, are reported to reside in the membrane of mammalian peroxisomes (1, 39, 40). The functional importance of these transporters is dem-

TABLE II

New candidates of mouse kidney peroxisomes identified by protein correlation profiling

N/A, no information available; Pex, peroxisomal.

Name	Gene name	IPI accession no.	Information on functional domains, transmembrane domains (TMDs), and further comments	PTS1 predicted by PSORT	Abundance by peptide scoring	Localization listed by UniProt	Localization by PCP
Zinc-binding alcohol dehydrogenase domain-containing protein 2[a]	*Zadh2*	00221569	Zinc-dependent oxidoreductase	Yes	5	N/A	Pex
Acyl-coenzyme A dehydrogenase family, member 11[a,b]	*Acad11*	00330747	N-terminal half: aminoglycoside phosphotransferase domain; C-terminal half: acyl-CoA dehydrogenase domain	Yes	54	N/A	Pex
2810439K08RIK protein[a]	*Tmem135*	00112089	Integral membrane protein of 52 kDa with 5 predicted TMDs (referred to as PMP52 in this work)	No	5	N/A	Pex
ACBD5 protein[a,b]	*Acbd5*	00229804	N-terminal half: acyl-CoA binding protein domain; may function as a carrier of acyl-CoA esters	No	8	N/A	Pex
ATPase family, AAA domain-containing protein 1	*Atad1*	00108410	Belongs to the AAA superfamily of ATPases; may perform chaperone-like functions to assist (dis)assembly and function of protein complexes	No	3	N/A	Pex
Abhydrolase domain-containing protein 14B	*Abhd14b*	00111876	N-terminal half: abhydrolase:lysophospholipase domain	No	4	N/A	Pex
RIKEN cDNA 1810022C23	N/A	00112190	78% similar to peroxisomal Δ^3,Δ^2-enoyl-CoA isomerase in *Mus musculus*; belongs to the enoyl-CoA hydratase/isomerase family	Yes	25	N/A	Pex
Multifunctional protein ADE2	*Paics*	00322096	N-terminal half: phosphoribosylaminoimidazole-succinocarboxamide synthase; C-terminal half: phosphoribosylaminoimidazole carboxylase; protein is involved in purine biosynthesis	No	2	Cytoplasmic	Pex
Acyl-CoA thioesterase 1	*Acot1*	00115871	N-terminal half: acyl-CoA thioester hydrolase and bile acid-CoA: amino acid *N*-acetyltransferase (BAAT); C-terminal half: dienelactone hydrolase; fulfills distinct functions in lipid metabolism; hydrolyzes bile acid-CoA esters in peroxisomes; induced in liver via proliferator-activated receptors	No	4	Cytoplasmic	Pex
Acyl-CoA thioester hydrolase 12	*Acot12*	00119810	N-terminal half: 2× brown fat-inducible thioesterase (BFIT) and brain acyl-CoA hydrolase (BACH); C-terminal half: steroidogenic acute regulatory-related lipid transfer (START) domain; involved in lipid transport and metabolism	No	18	Cytoplasmic	Pex
Malate dehydrogenase 1[b]	*Mdh1*	00336324	Member of the NAD-dependent 2-hydroxycarboxylate dehydrogenase family; involved in energy production and conversion	No	3	Cytoplasmic	Dual
Fatty aldehyde dehydrogenase variant form[b,c]	*Aldh3a2*	00111235	NAD-dependent aldehyde dehydrogenase domain; catalyzes the oxidation of fatty aldehydes to fatty acids; mutations in the Aldh3a2 gene cause the early childhood-onset disorder Sjögren-Larsson syndrome (SLS)	No	9	Microsomal	Pex
Cytochrome b_5[b,c]	*Cyb5A*	00230113	N-terminal half: cytochrome b_5-like heme/steroid-binding domain; involved in electron transport and fatty acid metabolism; may be membrane-anchored	No	4	Microsomal	Dual

TABLE II—*continued*

Name	Gene name	IPI accession no.	Information on functional domains, transmembrane domains (TMDs), and further comments	PTS1 predicted by PSORT	Abundance by peptide scoring	Localization listed by UniProt	Localization by PCP
NADH-cytochrome b_5 reductase homolog[b,c]	*Dia1*	00110885	N-terminal half: oxidoreductase FAD-binding domain; C-terminal half: oxidoreductase NAD-binding domain; involved in lipid metabolism	No	5	Microsomal	Dual
MOCO sulfurase C-terminal domain-containing 2[a]	*Mosc2*	00123276	Fe-S protein with 1 predicted TMD that contains a MOSC N-terminal β barrel domain and was found to be localized in the inner mitochondrial (60)	No	5	Mitochondrial	Dual

[a] Localization of proteins in peroxisomes was confirmed by fluorescence microscopy.
[b] Protein identified previously in rat liver peroxisomes by Kikuchi *et al.* (11).
[c] Protein identified previously in rat liver peroxisomes by Islinger *et al.* (12).

FIG. 2. **Validation of five candidates predicted to localize to peroxisomes by protein correlation profiling.** Shown are the immunofluorescence patterns of COS7 cells transiently expressing the proteins ACAD11-FLAG, EGFP-ZADH2, PMP52-EGFP, ACBD5-EGFP, and MOSC2-MYC labeled with α-FLAG, α-EGFP, or α-MYC antibodies. Peroxisomes are labeled with PMP70. Images from the *left* to the *right* are: respective candidate protein (*green*), PMP70 as peroxisomal marker protein (*red*), and merge. *Bottom panel*, MOSC2-MYC (*green*), MitoTracker (*red*), and merge (for further details please refer to the text).

onstrated by mutations in the *ALD* gene that encodes for ALDP causing X-linked adrenoleukodystrophy, an inherited neurodegenerative disorder in which saturated, very long-chain fatty acids accumulate because of impaired β-oxidation in peroxisomes (1, 39). Interestingly there is evidence that these ABC transporters show some functional redundancy, providing new possibilities for the treatment of X-linked adre-

noleukodystrophy patients (41–43). The expression of these membrane proteins was found to vary in different tissues (44). For example, a high level of PMP70 but very low ALDR expression was observed in mouse kidney as assessed by mRNA analysis (45). Using current proteomics methodologies, we could readily identify both PMP70 and ALDP in mouse kidney peroxisomes, whereas ALDR and PMP69 remained elusive. Because we successfully identified PMPs of very low abundance such as PEX13, we hypothesize that both ALDR and PMP69 show very low expression in mouse kidney peroxisomes. The inability to detect the peroxins PEX7 and PEX19 can be rationalized by their mainly cytosolic localization due to their function as shuttling receptor proteins (46, 47). If peripherally attached to the membrane, they are in all likelihood removed by carbonate treatment of peroxisome samples as performed in this work. Furthermore we did not detect the peroxisomal matrix proteins PTE1C, bile acid-CoA:amino acid *N*-acyltransferase (BACAT), polyamine oxidase, malonyl-CoA decarboxylase, MPV17, XDH, and NUDT7. The latter, peroxisomal nudix hydrolase 7, exhibits highest expression in liver but only intermediate expression in kidney (48). A similar pattern of expression was found for the human orthologue, NUDT7. However, NUDT7 as well as xanthine oxidoreductase, XDH (49), were not detected in peroxisomal preparations from rat liver by proteomics studies either (11, 12). Yet Kikuchi *et al.* (11) were able to detect BACAT, a member of the type I acyl-CoA thioesterases, in rat liver peroxisomes. BACAT was recently shown to be strongly expressed in liver, and moreover the human orthologue was mainly found in the cytosol (50, 51). Accordingly if expressed at all, BACAT may only be present in vanishing low amounts in mouse kidney peroxisomes. Furthermore low expression of the peroxisomal acyl-CoA thioesterase Ic (PTE1C) in kidney was reported (52), providing us with a reasonable explanation why this protein was not detected in this work.

Recent data initiated a new debate on the cellular localization of MPV17. Although Zwacka *et al.* (53) reported a role for MPV17 in the peroxisomal reactive oxygen metabolism, Spinazzola *et al.* (54) just recently demonstrated that this protein is an integral constituent of the mitochondrial inner membrane and that its absence or malfunction causes failure of oxidative phosphorylation. The latter investigation (54) supports proteomics data, *i.e.* the failure to detect MPV17 in preparations of mammalian peroxisomes as reported here and in previous studies (11, 12). Two further proteins were not detected in our study, N^1-acetylated polyamine oxidase exhibiting only low expression in kidney peroxisomes (55) as well as a putative peroxisomal form of malonyl-CoA decarboxylase (56). In view of the above discussion, we argue that we were able to detect virtually all known resident proteins of mouse kidney peroxisomes. This inventory also includes enzymes just recently designated as peroxisomal, such as the acyltransferase ACNAT1 (57), RP2 (13), and the Lon protease (11).

Through elaborate PCP combined with statistical analyses, we provided a set of 15 new peroxisomal candidates of which four proteins, namely ZADH2, ACAD11, ACBD5, and the RIKEN cDNA clone 2810439K08 (designated as PMP52), were validated by immunocytochemistry (Table II and Fig. 2). Six of these candidates (ACAD11, ACBD5, MDH1, CYB5A, DIA1, and ALDH3A2) were also detected in peroxisome preparations from rat liver (11, 12) (Table II). All new candidates identified here were of moderate to very low abundance as estimated by peptide counting, demonstrating the general capability of PCP to identify even minor organellar components against a background of contaminants. Failure to establish the profile of a given protein was usually due to the incapability to detect this compound in an adequate number of gradient fractions due to its low abundance. On the basis of our results, we estimate the false positive rate of protein localization by PCP to be lower than 10%, which is in agreement with previous studies (15, 17). Our work ultimately resulted in a significant increase in the number of peroxisomal proteins and we believe the most comprehensive, yet not complete, catalogue of mammalian peroxisomes.

To the best of our knowledge, no information about cellular localization is available for half of the 15 peroxisomal candidates identified in this work. Only four candidates (ZADH2, ACAD11, ABHD14B, and a protein similar to BACAT) contain a peroxisomal targeting signal type 1 (PTS1) as predicted by using PSORT (58). For ZADH2 and ACAD11 we also showed by fluorescence microscopy that they localize to peroxisomes and thus contain a functional peroxisomal targeting signal.

Of great interest is the identification of PMP52, which is related to PMP24, a *bona fide* component of the peroxisomal membrane (59). Localization of PMP52 to peroxisomes was shown by both PCP and immunofluorescence. Consequently we suggest that PMP52 represents a new integral component of peroxisomal membranes that may have functions similar to those of PMP24. Apart from PMP52, two additional components of the peroxisomal membrane were identified, MOSC2 and ATAD1. MOSC2 was shown to exhibit a dual localization based on PCP as well as immunofluorescence spectroscopy in this study; as yet, however, this iron-sulfur protein was known to be exclusively localized to mitochondria (60). ATAD1 belongs to the AAA superfamily of ATPases. Most members of this functionally diverse group of enzymes are involved in the unfolding of proteins or disassembly of protein complexes and aggregates (for a review, see Ref. 61), a property that could suggest that ATAD1 is involved in some aspects of peroxisomal homeostasis. We note, however, that whatever the physiological role of ATAD1 is, it may not be restricted to peroxisomes only. Indeed transient expression of an ATAD1-green fluorescent protein fusion protein in mammalian cells revealed a peroxisomal and mitochondrial localization. This observation is in general agreement with the finding that MSP1 (a yeast protein displaying 51% sequence identity to ATAD1) displays the same behavior.[2] Yeast MSP1 was first

[2] R. Erdmann, W. Schliebs, and W. Girzalsky, unpublished data.

described by Nakai *et al.* (62) as a protein involved in intramitochondrial protein sorting. We also provided first evidence for the peroxisomal localization of the two acyl-CoA thioesterases ACOT1 and ACOT12 as well as the multifunctional protein ADE2. As yet, these enzymes were considered to reside in the cytoplasm. Because ACOT1 and ACOT12 are members of a group of enzymes that hydrolyze CoA esters to the corresponding free acids and CoA (63, 64), they are suggested to be involved in the regulation of lipid metabolism. ACOT1 was recently reported to exhibit high specificity for C_{12} to C_{20} acyl-CoA esters with a high activity in the cytosol (65). Our data, however, show that ACOT1 is most likely present in peroxisomes as well.

The localization studies performed in this work confirm previous reports (11, 12, 66, 67) that suggest the peroxisomal localization of three microsomal proteins, namely cytochrome b_5 (CYB5A), the corresponding reductase (DIA1), and the fatty aldehyde dehydrogenase (FALDH) encoded by the gene *Aldh3a2*. Although for the first two microsomal proteins a dual localization was assigned by PCP, our profiling data indicate an association of the FALDH with peroxisomes. In view of this finding, it is tempting to suggest an important role for FALDH in lipid metabolism (*e.g.* the detoxification of fatty aldehydes) in peroxisomes. At this point, it is also of great interest to note that mutations in the *Aldh3a2* gene cause Sjögren-Larsson syndrome, an inherited human neurocutaneous disorder characterized by ichthyosis, mental retardation, and spasticity. The pathogenesis of these symptoms is thought to result from abnormal lipid accumulation, defective metabolism of eicosanoids, or the increased formation of aldehyde adducts with lipids and/or proteins (68, 69).

CONCLUDING REMARKS

Using a quantitative MS-based screen, we identified 15 new peroxisomal candidate proteins, including three putative membrane proteins. To increase the possibility of identifying new integral membrane components of peroxisomes, we advocate the idea of subjecting density gradient fractions enriched for membranes to PCP analysis. The detection of 15 new candidates, of which five proteins were validated by immunofluorescence microscopy, opens up the possibility to gain new insight into peroxisomal functions in health and disease. In our research alliance, follow-up studies on new peroxisomal proteins reported in this work have already been initiated for functional characterization. This may eventually result in a better understanding of the biochemistry of mammalian peroxisomes as well as the improvement of our knowledge about human diseases linked to the malfunction of peroxisomes.

Acknowledgments—We are grateful to Prof. Werner Sieghart for providing rabbit antibodies against EGFP; Prof. Gerrit Jansen for expert knowledge assistance; Nadine Stoepel, Magdalena Pawlas, and Christian Bunse for technical assistance; and Dr. Silke Oeljeklaus for critically reading the manuscript.

* This work was supported by the FP6 European Union Project "Peroxisome" (Grant LSHG-CT-2004-512018), by funds from the German Federal Ministry for Education and Research, the Deutsche Forschungsgemeinschaft, and by the Austrian science fund (Grant FWF-P15510-B14). The costs of publication of this article were defrayed in part by the payment of page charges. This article must therefore be hereby marked "*advertisement*" in accordance with 18 U.S.C. Section 1734 solely to indicate this fact.

S The on-line version of this article (available at http://www.mcponline.org) contains supplemental material.

§ Both authors contributed equally to this work.

|||| To whom correspondence should be addressed. Tel.: 49-0234-32-29266; Fax: 49-0234-32-14554; E-mail: Bettina.Warscheid@rub.de.

REFERENCES

1. Wanders, R. J., and Waterham, H. R. (2006) Biochemistry of mammalian peroxisomes revisited. *Annu. Rev. Biochem.* **75,** 295–332
2. Heiland, I., and Erdmann, R. (2005) Biogenesis of peroxisomes. Topogenesis of the peroxisomal membrane and matrix proteins. *FEBS J.* **272,** 2362–2372
3. Brown, L. A., and Baker, A. (2003) Peroxisome biogenesis and the role of protein import. *J. Cell. Mol. Med.* **7,** 388–400
4. Yates, J. R., III, Gilchrist, A., Howell, K. E., and Bergeron, J. J. (2005) Proteomics of organelles and large cellular structures. *Nat. Rev. Mol. Cell Biol.* **6,** 702–714
5. Andersen, J. S., and Mann, M. (2006) Organellar proteomics: turning inventories into insights. *EMBO Rep.* **7,** 874–879
6. Dreger, M. (2003) Subcellular proteomics. *Mass Spectrom. Rev.* **22,** 27–56
7. Saleem, R. A., Smith, J. J., and Aitchison, J. D. (2006) Proteomics of the peroxisome. *Biochim. Biophys. Acta* **1763,** 1541–1551
8. Schafer, H., Nau, K., Sickmann, A., Erdmann, R., and Meyer, H. E. (2001) Identification of peroxisomal membrane proteins of *Saccharomyces cerevisiae* by mass spectrometry. *Electrophoresis* **22,** 2955–2968
9. Yi, E. C., Marelli, M., Lee, H., Purvine, S. O., Aebersold, R., Aitchison, J. D., and Goodlett, D. R. (2002) Approaching complete peroxisome characterization by gas-phase fractionation. *Electrophoresis* **23,** 3205–3216
10. Marelli, M., Smith, J. J., Jung, S., Yi, E., Nesvizhskii, A. I., Christmas, R. H., Saleem, R. A., Tam, Y. Y., Fagarasanu, A., Goodlett, D. R., Aebersold, R., Rachubinski, R. A., and Aitchison, J. D. (2004) Quantitative mass spectrometry reveals a role for the GTPase Rho1p in actin organization on the peroxisome membrane. *J. Cell Biol.* **167,** 1099–1112
11. Kikuchi, M., Hatano, N., Yokota, S., Shimozawa, N., Imanaka, T., and Taniguchi, H. (2004) Proteomic analysis of rat liver peroxisome: presence of peroxisome-specific isozyme of Lon protease. *J. Biol. Chem.* **279,** 421–428
12. Islinger, M., Luers, G. H., Zischka, H., Ueffing, M., and Volkl, A. (2006) Insights into the membrane proteome of rat liver peroxisomes: microsomal glutathione-S-transferase is shared by both subcellular compartments. *Proteomics* **6,** 804–816
13. Ofman, R., Speijer, D., Leen, R., and Wanders, R. J. (2006) Proteomic analysis of mouse kidney peroxisomes: identification of RP2p as a peroxisomal nudix hydrolase with acyl-CoA diphosphatase activity. *Biochem. J.* **393,** 537–543
14. Dunkley, T. P., Dupree, P., Watson, R. B., and Lilley, K. S. (2004) The use of isotope-coded affinity tags (ICAT) to study organelle proteomes in *Arabidopsis thaliana*. *Biochem. Soc. Trans.* **32,** 520–523
15. Andersen, J. S., Wilkinson, C. J., Mayor, T., Mortensen, P., Nigg, E. A., and Mann, M. (2003) Proteomic characterization of the human centrosome by protein correlation profiling. *Nature* **426,** 570–574
16. Gilchrist, A., Au, C. E., Hiding, J., Bell, A. W., Fernandez-Rodriguez, J., Lesimple, S., Nagaya, H., Roy, L., Gosline, S. J., Hallett, M., Paiement, J., Kearney, R. E., Nilsson, T., and Bergeron, J. J. (2006) Quantitative proteomics analysis of the secretory pathway. *Cell* **127,** 1265–1281
17. Foster, L. J., de Hoog, C. L., Zhang, Y., Zhang, Y., Xie, X., Mootha, V. K., and Mann, M. (2006) A mammalian organelle map by protein correlation profiling. *Cell* **125,** 187–199
18. Dunkley, T. P., Hester, S., Shadforth, I. P., Runions, J., Weimar, T., Hanton, S. L., Griffin, J. L., Bessant, C., Brandizzi, F., Hawes, C., Watson, R. B., Dupree, P., and Lilley, K. S. (2006) Mapping the *Arabidopsis* organelle proteome. *Proc. Natl. Acad. Sci. U. S. A.* **103,** 6518–6523

19. Lilley, K. S., and Dupree, P. (2006) Methods of quantitative proteomics and their application to plant organelle characterization. *J. Exp. Bot.* **57,** 1493–1499
20. Wanders, R. J., van Roermund, C. W., Schor, D. S., ten Brink, H. J., and Jakobs, C. (1994) 2-Hydroxyphytanic acid oxidase activity in rat and human liver and its deficiency in the Zellweger syndrome. *Biochim. Biophys. Acta* **1227,** 177–182
21. Bradford, M. M. (1976) A rapid and sensitive method for the quantitation of microgram quantities of protein utilizing the principle of protein-dye binding. *Anal. Biochem.* **72,** 248–254
22. Fujiki, Y., Fowler, S., Shio, H., Hubbard, A. L., and Lazarow, P. B. (1982) Polypeptide and phospholipid composition of the membrane of rat liver peroxisomes: comparison with endoplasmic reticulum and mitochondrial membranes. *J. Cell Biol.* **93,** 103–110
23. Wanders, R. J., Dekker, C., Ofman, R., Schutgens, R. B., and Mooijer, P. (1995) Immunoblot analysis of peroxisomal proteins in liver and fibroblasts from patients. *J. Inherit. Metab. Dis.* **18,** Suppl. 1, 101–112
24. Ferdinandusse, S., Denis, S., L, I. J., Dacremont, G., Waterham, H. R., and Wanders, R. J. (2000) Subcellular localization and physiological role of α-methylacyl-CoA racemase. *J. Lipid Res.* **41,** 1890–1896
25. Schaefer, H., Chervet, J. P., Bunse, C., Joppich, C., Meyer, H. E., and Marcus, K. (2004) A peptide preconcentration approach for nano-high-performance liquid chromatography to diminish memory effects. *Proteomics* **4,** 2541–2544
26. Olsen, J. V., Ong, S. E., and Mann, M. (2004) Trypsin cleaves exclusively C-terminal to arginine and lysine residues. *Mol. Cell. Proteomics* **3,** 608–614
27. Perkins, D. N., Pappin, D. J., Creasy, D. M., and Cottrell, J. S. (1999) Probability-based protein identification by searching sequence databases using mass spectrometry data. *Electrophoresis* **20,** 3551–3567
28. Stephan, C., Reidegeld, K. A., Hamacher, M., van Hall, A., Marcus, K., Taylor, C., Jones, P., Muller, M., Apweiler, R., Martens, L., Korting, G., Chamrad, D. C., Thiele, H., Bluggel, M., Parkinson, D., Binz, P. A., Lyall, A., and Meyer, H. E. (2006) Automated reprocessing pipeline for searching heterogeneous mass spectrometric data of the HUPO Brain Proteome Project pilot phase. *Proteomics* **6,** 5015–5029
29. Yates, J. R., III, Eng, J. K., McCormack, A. L., and Schieltz, D. (1995) Method to correlate tandem mass spectra of modified peptides to amino acid sequences in the protein database. *Anal. Chem.* **67,** 1426–1436
30. Hartigan, J. A., and Wong, M. A. (1979) Algorithm AS136: a k-means clustering algorithm. *Appl. Stat.* **28,** 100–108
31. Mosser, J., Lutz, Y., Stoeckel, M. E., Sarde, C. O., Kretz, C., Douar, A. M., Lopez, J., Aubourg, P., and Mandel, J. L. (1994) The gene responsible for adrenoleukodystrophy encodes a peroxisomal membrane protein. *Hum. Mol. Genet.* **3,** 265–271
32. Iida, R., Yasuda, T., Tsubota, E., Matsuki, T., and Kishi, K. (2001) Cloning, mapping, genomic organization, and expression of mouse M-LP, a new member of the peroxisomal membrane protein Mpv17 domain family. *Biochem. Biophys. Res. Commun.* **283,** 292–296
33. Bjorkman, J., Stetten, G., Moore, C. S., Gould, S. J., and Crane, D. I. (1998) Genomic structure of PEX13, a candidate peroxisome biogenesis disorder gene. *Genomics* **54,** 521–528
34. Shimozawa, N., Tsukamoto, T., Suzuki, Y., Orii, T., Shirayoshi, Y., Mori, T., and Fujiki, Y. (1992) A human gene responsible for Zellweger syndrome that affects peroxisome assembly. *Science* **255,** 1132–1134
35. Reguenga, C., Oliveira, M. E., Gouveia, A. M., Sa-Miranda, C., and Azevedo, J. E. (2001) Characterization of the mammalian peroxisomal import machinery: Pex2p, Pex5p, Pex12p, and Pex14p are subunits of the same protein assembly. *J. Biol. Chem.* **276,** 29935–29942
36. Gouveia, A. M., Reguenga, C., Oliveira, M. E., Eckerskorn, C., Sa-Miranda, C., and Azevedo, J. E. (1999) Alkaline density gradient floatation of membranes: polypeptide composition of the mammalian peroxisomal membrane. *Anal. Biochem.* **274,** 270–277
37. Tanaka, A. R., Tanabe, K., Morita, M., Kurisu, M., Kasiwayama, Y., Matsuo, M., Kioka, N., Amachi, T., Imanaka, T., and Ueda, K. (2002) ATP binding/hydrolysis by and phosphorylation of peroxisomal ATP-binding cassette proteins PMP70 (ABCD3) and adrenoleukodystrophy protein (ABCD1). *J. Biol. Chem.* **277,** 40142–40147
38. Liu, H., Sadygov, R. G., and Yates, J. R., III (2004) A model for random sampling and estimation of relative protein abundance in shotgun proteomics. *Anal. Chem.* **76,** 4193–4201
39. Theodoulou, F. L., Holdsworth, M., and Baker, A. (2006) Peroxisomal ABC transporters. *FEBS Lett.* **580,** 1139–1155
40. Wanders, R. J., Visser, W. F., van Roermund, C. W., Kemp, S., and Waterham, H. R. (2007) The peroxisomal ABC transporter family. *Pfluegers Arch. Eur. J. Physiol.***453,** 719–734
41. Kemp, S., and Wanders, R. J. (2007) X-linked adrenoleukodystrophy: very long-chain fatty acid metabolism, ABC half-transporters and the complicated route to treatment. *Mol. Genet. Metab.* **90,** 268–276
42. Kemp, S., Wei, H. M., Lu, J. F., Braiterman, L. T., McGuinness, M. C., Moser, A. B., Watkins, P. A., and Smith, K. D. (1998) Gene redundancy and pharmacological gene therapy: implications for X-linked adrenoleukodystrophy. *Nat. Med.* **4,** 1261–1268
43. Netik, A., Forss-Petter, S., Holzinger, A., Molzer, B., Unterrainer, G., and Berger, J. (1999) Adrenoleukodystrophy-related protein can compensate functionally for adrenoleukodystrophy protein deficiency (X-ALD): implications for therapy. *Hum. Mol. Genet.* **8,** 907–913
44. Smith, K. D., Kemp, S., Braiterman, L. T., Lu, J. F., Wei, H. M., Geraghty, M., Stetten, G., Bergin, J. S., Pevsner, J., and Watkins, P. A. (1999) X-linked adrenoleukodystrophy: genes, mutations, and phenotypes. *Neurochem. Res.* **24,** 521–535
45. Berger, J., Albet, S., Bentejac, M., Netik, A., Holzinger, A., Roscher, A. A., Bugaut, M., and Forss-Petter, S. (1999) The four murine peroxisomal ABC-transporter genes differ in constitutive, inducible and developmental expression. *Eur. J. Biochem.* **265,** 719–727
46. Sacksteder, K. A., Jones, J. M., South, S. T., Li, X., Liu, Y., and Gould, S. J. (2000) PEX19 binds multiple peroxisomal membrane proteins, is predominantly cytoplasmic, and is required for peroxisome membrane synthesis. *J. Cell Biol.* **148,** 931–944
47. Rehling, P., Marzioch, M., Niesen, F., Wittke, E., Veenhuis, M., and Kunau, W. H. (1996) The import receptor for the peroxisomal targeting signal 2 (PTS2) in *Saccharomyces cerevisiae* is encoded by the PAS7 gene. *EMBO J.* **15,** 2901–2913
48. Gasmi, L., and McLennan, A. G. (2001) The mouse Nudt7 gene encodes a peroxisomal nudix hydrolase specific for coenzyme A and its derivatives. *Biochem. J.* **357,** 33–38
49. Terao, M., Cazzaniga, G., Ghezzi, P., Bianchi, M., Falciani, F., Perani, P., and Garattini, E. (1992) Molecular cloning of a cDNA coding for mouse liver xanthine dehydrogenase. Regulation of its transcript by interferons in vivo. *Biochem. J.* **283,** 863–870
50. Solaas, K., Kase, B. F., Pham, V., Bamberg, K., Hunt, M. C., and Alexson, S. E. (2004) Differential regulation of cytosolic and peroxisomal bile acid amidation by PPAR α activation favors the formation of unconjugated bile acids. *J. Lipid Res.* **45,** 1051–1060
51. O'Byrne, J., Hunt, M. C., Rai, D. K., Saeki, M., and Alexson, S. E. (2003) The human bile acid-CoA:amino acid N-acyltransferase functions in the conjugation of fatty acids to glycine. *J. Biol. Chem.* **278,** 34237–34244
52. Westin, M. A., Alexson, S. E., and Hunt, M. C. (2004) Molecular cloning and characterization of two mouse peroxisome proliferator-activated receptor α (PPARα)-regulated peroxisomal acyl-CoA thioesterases. *J. Biol. Chem.* **279,** 21841–21848
53. Zwacka, R. M., Reuter, A., Pfaff, E., Moll, J., Gorgas, K., Karasawa, M., and Weiher, H. (1994) The glomerulosclerosis gene Mpv17 encodes a peroxisomal protein producing reactive oxygen species. *EMBO J.* **13,** 5129–5134
54. Spinazzola, A., Viscomi, C., Fernandez-Vizarra, E., Carrara, F., D'Adamo, P., Calvo, S., Marsano, R. M., Donnini, C., Weiher, H., Strisciuglio, P., Parini, R., Sarzi, E., Chan, A., DiMauro, S., Rotig, A., Gasparini, P., Ferrero, I., Mootha, V. K., Tiranti, V., and Zeviani, M. (2006) MPV17 encodes an inner mitochondrial membrane protein and is mutated in infantile hepatic mitochondrial DNA depletion. *Nat. Genet.* **38,** 570–575
55. Wu, T., Yankovskaya, V., and McIntire, W. S. (2003) Cloning, sequencing, and heterologous expression of the murine peroxisomal flavoprotein, N^1-acetylated polyamine oxidase. *J. Biol. Chem.* **278,** 20514–20525
56. Sacksteder, K. A., Morrell, J. C., Wanders, R. J., Matalon, R., and Gould, S. J. (1999) MCD encodes peroxisomal and cytoplasmic forms of malonyl-CoA decarboxylase and is mutated in malonyl-CoA decarboxylase deficiency. *J. Biol. Chem.* **274,** 24461–24468
57. Reilly, S. J., O'Shea, E. M., Andersson, U., O'Byrne, J., Alexson, S. E., and Hunt, M. C. (2007) A peroxisomal acyltransferase in mouse identifies a novel pathway for taurine conjugation of fatty acids. *FASEB J.* **21,** 99–107

58. Nakai, K., and Horton, P. (1999) PSORT: a program for detecting sorting signals in proteins and predicting their subcellular localization. *Trends Biochem. Sci.* **24,** 34–36
59. Reguenga, C., Oliveira, M. E., Gouveia, A. M., Eckerskorn, C., Sa-Miranda, C., and Azevedo, J. E. (1999) Identification of a 24 kDa intrinsic membrane protein from mammalian peroxisomes. *Biochim. Biophys. Acta* **1445,** 337–341
60. Da Cruz, S., Xenarios, I., Langridge, J., Vilbois, F., Parone, P. A., and Martinou, J. C. (2003) Proteomic analysis of the mouse liver mitochondrial inner membrane. *J. Biol. Chem.* **278,** 41566–41571
61. Hanson, P. I., and Whiteheart, S. W. (2005) AAA+ proteins: have engine, will work. *Nat. Rev. Mol. Cell Biol.* **6,** 519–529
62. Nakai, M., Endo, T., Hase, T., and Matsubara, H. (1993) Intramitochondrial protein sorting. Isolation and characterization of the yeast MSP1 gene which belongs to a novel family of putative ATPases. *J. Biol. Chem.* **268,** 24262–24269
63. Hunt, M. C., and Alexson, S. E. (2002) The role Acyl-CoA thioesterases play in mediating intracellular lipid metabolism. *Prog. Lipid Res.* **41,** 99–130
64. Hunt, M. C., Yamada, J., Maltais, L. J., Wright, M. W., Podesta, E. J., and Alexson, S. E. (2005) A revised nomenclature for mammalian acyl-CoA thioesterases/hydrolases. *J. Lipid Res.* **46,** 2029–2032
65. Huhtinen, K., O'Byrne, J., Lindquist, P. J., Contreras, J. A., and Alexson, S. E. (2002) The peroxisome proliferator-induced cytosolic type I acyl-CoA thioesterase (CTE-I) is a serine-histidine-aspartic acid α/β hydrolase. *J. Biol. Chem.* **277,** 3424–3432
66. Miyauchi, K., Yamamoto, A., Masaki, R., Fujiki, Y., and Tashiro, Y. (1993) Microsomal aldehyde dehydrogenase or its cross-reacting protein exists in outer mitochondrial membranes and peroxisomal membranes in rat liver. *Cell Struct. Funct.* **18,** 427–436
67. Fowler, S., Remacle, J., Trouet, A., Beaufay, H., Berthet, J., Wibo, M., and Hauser, P. (1976) Analytical study of microsomes and isolated subcellular membranes from rat liver. V. Immunological localization of cytochrome b5 by electron microscopy: methodology and application to various subcellular fractions. *J. Cell Biol.* **71,** 535–550
68. Rizzo, W. B., and Carney, G. (2005) Sjogren-Larsson syndrome: diversity of mutations and polymorphisms in the fatty aldehyde dehydrogenase gene (ALDH3A2). *Hum. Mutat.* **26,** 1–10
69. Gordon, N. (2007) Sjogren-Larsson syndrome. *Dev. Med. Child Neurol.* **49,** 152–154